

# Photocatalytic activity of nanostructured TiO<sub>2</sub> thin films prepared by pulsed spray pyrolysis

Alcides López<sup>1,2,3</sup> [alopez@ipen.gob.pe](mailto:alopez@ipen.gob.pe), Dwight Acosta<sup>1</sup>, Arturo Martínez<sup>1</sup>

<sup>1</sup> Thin Films Laboratory, Condensed Matter Department, Universidad Nacional Autónoma de México A.P. 20-364; 01000 México D.F., México

<sup>2</sup> Instituto Peruano de Energía Nuclear Av. Canadá 1470, Lima, Perú

<sup>3</sup> Universidad Nacional de Ingeniería, P. O. Box 31-139, Av. Túpac Amaru 210, Lima, Perú

## Abstract

Nano-structured TiO<sub>2</sub> thin films were deposited onto soda lime glass by the pneumatic spray pyrolysis method from a peroxo-titanium complex solution. Samples were prepared spraying 10 s the complex solution followed by an interruption of 20 s in order to avoid inadequate substrate cooling, the substrate temperature was varied from 230 to 430 °C in 50 °C steps. Amorphous as-deposited films crystallized to the anatase phase after an annealing process at 500 °C for 3 h. The photocatalytic activity of the nanostructured TiO<sub>2</sub> thin films was studied under UV irradiation with the degradation of methylene-blue. Amorphous as-deposited TiO<sub>2</sub> films prepared at low substrate temperatures (280 °C) showed the best photocatalytic activity, but after the annealing process films exhibit a decrease in the photocatalytic activity due to both the increase in the grain size and the decrease in the surface area.

Keywords: TiO<sub>2</sub> Thin Films; Spray Pyrolysis; Methylene blue; Photocatalyst

## 1. Introduction

Titanium dioxide is a wide band gap semiconductor with interesting chemical, electrical and optical properties [1, 2]. Nanoparticles and nanostructured TiO<sub>2</sub> thin films have been extensively studied in photocatalysis [3-5], electrochromism [6], gas sensing [7], etc. Photocatalytic degradation of organic compounds has been proposed as viable alternative to decontaminate either waste water or drinking water [1]. Nanostructured TiO<sub>2</sub> shows improved photocatalytic behaviour because of its greater specific surface area than conventional coarse-grained TiO<sub>2</sub> [3-5]. However, there is a drawback with TiO<sub>2</sub>-nanoparticles when used in photocatalytic processes because it is not easy to remove from the degraded solution by centrifugation and filtration processes. Many alternatives have been proposed to overcome this limitation; for example, nanoparticles of titanium dioxide photocatalyst anchored or embedded onto support materials with large surface areas have been tested. These nanoparticles have been immobilized onto supports such as glass surface [8], polymer latex particles [9], high-surface-area ceramic hollow spheres [10] and activated carbon [11]. A number of methods have been reported for the preparation of TiO<sub>2</sub> thin films, including chemical vapor deposition [12], flame spraying [13], laser ablation [14], sol gel [15,16], sputtering [17-19], electron beam evaporation [20], hydrolysis by organo metallic route [21], reactive evaporation [22], spray pyrolysis (SP) [23-29], etc. Among

these techniques, SP is one of the most simple and inexpensive technique for different applications and can be easily use to coat large-surface areas with homogeneous properties. The precursor solution to prepare TiO<sub>2</sub> thin film by the SP technique mostly uses titanium(IV) organometallic compounds, such as Ti-tetra-ethoxide, Ti iso-propoxide, Ti isobutoxide, and Ti acetylacetonate in non-aqueous solvents; also, those compounds are expensive and release toxic products to environment after film deposition. Natarajan et al. [29] reported the TiO<sub>2</sub> film deposition by the SP method using a peroxo-titanium complex diluted in water for Li ion battery applications that is cheap and don't release toxic by products. Our main interest is to prepare titanium dioxide thin films with structural, optical and electronic characteristics suitable for photocatalytic applications, on the other hand, as a first step to produce supported oxide compounds, specially avoiding to release toxic products to the environment.

In this paper, we report the synthesis of peroxo-titanium complex solution and the preparation of transparent photocatalytic TiO<sub>2</sub> thin films onto soda-lime glass by SP method using this solution. The influence of the deposition temperature and the annealing conditions on the structural properties of TiO<sub>2</sub> films and the photocatalytic degradation of methylene blue under UV irradiation was systematically studied and discussed.

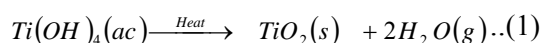
## 2. Experimental

### 2.1 Film deposition

The TiO<sub>2</sub> thin films were deposited using a conventional pneumatic spray pyrolysis system [30]. The spraying solution was prepared dissolving 0.450 g of titanium metal powder (100 mesh, 99% from Aldrich) in 53 ml 30% hydrogen peroxide and 2 ml of ammonia solution (J. T. Baker); the dissolution was completed in 3 h becoming a transparent yellow solution. This was under bubbling for 3 days and a 30 ml of hydrogen peroxide mixed with 255 ml of ethanol (Merck) were added to the solution, followed by 6 ml of HCl 36.8%; a 0.212 M concentration of HCl was obtained and kept constant in the solution during the synthesis of peroxo-titanium complex solution.

The solution prepared as described above was sprayed onto a hot 25 × 25 × 1 mm<sup>3</sup> soda-lime glass substrate previous ultrasonically cleaned with soap, acetone and methyl alcohol. The temperature of the hot plate was controlled within ± 5 °C and the substrate temperature,  $T_s$ , was varied from 230 to 430 °C in 50 °C steps. The deposition was performed using compressed filtered and dehydrated air as carrier gas; kept at 12.4 l/min and 170 kPa. The spraying process consists in: a spraying of 10 s followed by an interruption of 20 s in order to avoid inadequate substrate cooling during the preparation. The as-deposited films were annealed in air at 500 °C for 3 h. The deposition time was carefully controlled in order to have films with a thickness around 400 nm.

When the aerosol droplets arrive close to the heated substrate a pyrolytic process is produced and a highly adherent film of TiO<sub>2</sub> develops according to the following reaction:



### 2.2 Morphology and structure

The thickness and roughness of the sprayed titanium dioxide thin films were measured using a Dektak IIA profilometer on the step formed during deposition with a standard scan length of 3000 μm. Spectral transmittance for TiO<sub>2</sub> films were recorded in the 290 < λ < 1100 nm wavelength range using an Agilent 8453 spectrophotometer.

The crystalline structures of as-deposited and annealed samples were characterized by X-ray diffraction (XRD) using a Bruker AXS D8 Advance X-ray diffractometer with Cu K<sub>α</sub> radiation (1.54056 Å). The surface morphology of the films were studied by

scanning electron microscopy (SEM) using a Jeol JSM 5200 CX instrument. The microstructure and grain size distribution of the films were carried out using a conventional TEM, Jeol 100 CX; the films were peeled off from the glass substrate scratching with a stainless steel knife, and the small flakes were floated in deionized water. They were mounted on 100 mesh carbon coated copper grids to be finally mounted in the TEM column.

### 2.3 Photoactivity measurements.

A methylene-blue (MB) dissolved in water was used in order to study the photocatalytic activity of both as-deposited and annealed TiO<sub>2</sub> films. The home-made photoreactor is shown schematically in Fig. 1; was used for in door experiments a 150 W Hg lamp placed 30 cm above the film. Photocatalytic efficiencies were evaluated irradiating during 6 h a 25 ml of a 20 ppm methylene-blue solution flowing over a 4 cm<sup>2</sup> of titanium dioxide thin film (see Fig. 1). The radiation intensity on the surface coating of TiO<sub>2</sub> close to ~ 18 mW/cm<sup>2</sup> was measured with a Spectra-Physics radiometer model 404. The solution was flowing on the TiO<sub>2</sub> thin film (Fig. 1) in a stationary regime controlled using a peristaltic pump, 2 ml of the MB solution was collected each 2 h from the photoreactor vessel and measured the methylene-blue concentration by the optical absorption at 656 nm wavelength [31] using an Agilent 8453 spectrophotometer, the solution was returned immediately after this measurement. 6 % of methylene-blue solution was photodegraded just UV irradiating in the absence of TiO<sub>2</sub> film; the photocatalytic activity measurements reported in this paper take into account this value for correction. The rate constants  $k$  and  $k_s$  (pseudo-first order rate constant per unit of surface area) for MB decomposition reaction was determined from the linear relationship between the logarithm of relative concentration of MB with the irradiation time [8, 31].

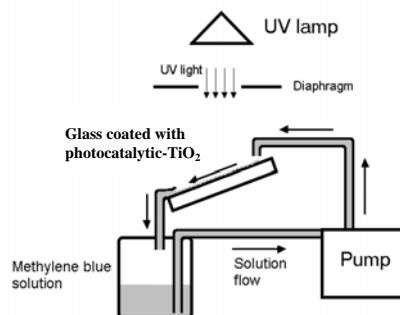


**Figure 1.** Schematic diagram of the photocatalytic reactor.

### 3. Results and discussion

#### 3.1 Morphology and structure

The thicknesses for all the samples of the as-deposited TiO<sub>2</sub> films were around 400 nm from profilometer measurements. Also the roughness for both as-deposited and annealed TiO<sub>2</sub> films as a function of the substrate temperature,  $T_s$ , are presented in Fig. 2.

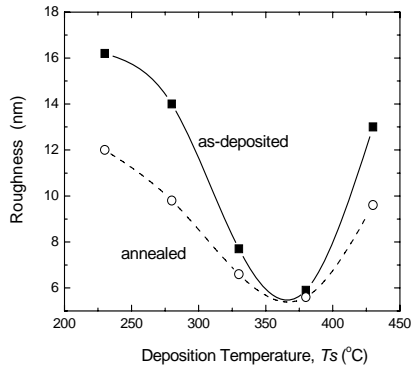


**Figure 2.** Surface roughness as a function of the deposition temperature,  $T_s$ , for as-deposited (■) and annealed at 500 °C for 3 h (○) TiO<sub>2</sub> films. Symbols denote data and the curves were drawn for convenience.

From the results it is found that the surface roughness is related to the deposition temperature; in fact, the root-mean-square (rms) roughness of the samples obtained with a substrate temperature between 230 and 380 °C decreases as a function of  $T_s$  (rms roughness of 16 nm for  $T_s=230$  °C and 6 nm for  $T_s=380$  °C). The fact can be explained by considering that a given substrate temperature the deposition of films is carried out by a real chemical vapor deposition process through heterogeneous chemical reactions, then the film is growing by an atomistic process. At higher  $T_s$  the adsorbed radicals have higher surface mobility resulting in a better accommodation and in a smoother surface of the deposited film. On the other hand, when a sample was additionally annealed at 500 °C for 3h in air atmosphere is induced the phase transformation, which implies a significant increase on the density and the grain growth effects [32].

Figure 3a shows SEM images of the surface of as-deposited TiO<sub>2</sub> thin films prepared varying  $T_s$  between 230 to 430 °C, on glass substrate, figure 3b shows SEM images for the surface of the same samples of figure 3a annealed at 500 °C for 3 h in air atmosphere. Films with smoother surfaces are obtained at  $T_s=330$  and  $T_s=380$  °C, which is coherent with results showed in figure 2 and the respective discussion. Between the as-deposited and annealed films there is a

slightly difference. The as-deposited and annealed TiO<sub>2</sub> films obtained with  $T_s=280$  °C show some cracks with consequent high chemisorptions level (due to the increase the surface places with greater coordination number [33]). From the X-ray measurements it was observed (in figure 4a) that samples of as-deposited TiO<sub>2</sub> thin films prepared varying  $T_s$  between 230 to 430 °C are amorphous. This result is in agreement with the non-crystalline structure obtained and reported for deposition temperatures below 400 °C [34], for  $T_s=430$  °C also can be seen a small peak around 25° from 2 $\theta$  corresponding to anatase phase. The X-ray measurements from samples annealed at 500 °C for 3 h in air atmosphere corresponds to the polycrystalline microstructure of anatase phase (JCPDS card 21-1272) as shown in figure 4b. In all these cases the peak with the highest intensity is associated with reflection from the (101) family planes. The main characteristic in those spectra is the low intensity of the diffraction peak and the mean grain size obtained by Scherrer's equation from  $T_s=230$  to 380 °C and  $T_s=430$  °C are around 5.0 nm and 5.25 nm, respectively. The initial small amount of anatase with a peak for (101) family plane change to the weak peak (211) reducing its crystalline property, this can interpreted as a loss of crystalline properties of the material in agreement with the phase change from anatase-TiO<sub>2</sub>-II that can be obtained only in laboratory [35]. (the TiO<sub>2</sub>-II structure has the same non-crystalline structure of  $\alpha$ -PbO<sub>2</sub>).

The TEM bright field micrographs and selected area electron diffraction (SAED) patterns for as-deposited and annealed TiO<sub>2</sub> films are shown in Fig. 5. The as-deposited films have basically a non-crystalline configuration; except some small amounts of brookite crystalline phase (JCPDS card 29-1360) were identified in a non-crystalline background (Fig. 5a), also we can observe that the small amount of the crystalline structure increase as a function of the substrate temperature  $T_s$ . The grain size measured from TEM micrographs for the as-deposited TiO<sub>2</sub> thin films prepared varying  $T_s$  between 230 to 380 °C were around 7.5 nm, and for  $T_s=430$  °C was around 15 nm. The annealed TiO<sub>2</sub> films revealed polycrystalline anatase phase (JCPDS) card 21-1272) with an average grain size of 10 nm measured from thin films prepared varying  $T_s$  between 230 to 380°C (Fig. 5b), for  $T_s=430$  °C the grain size was close to 20 nm. From the SAED patterns and the grain size observed it observed that thermal treatment induced crystallization promoted the grain growth, which reduce the effective surface area.

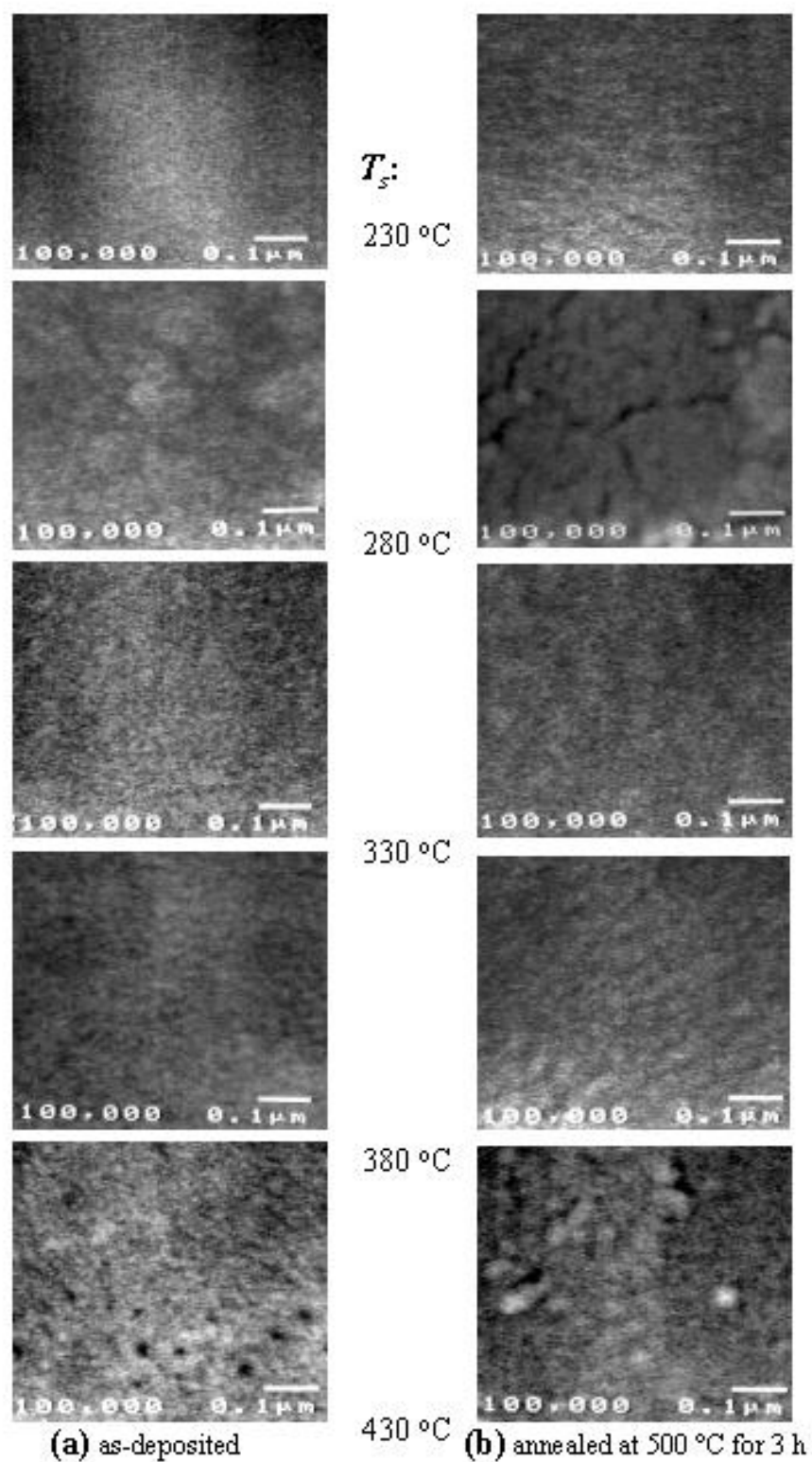


**Figure 3.** SEM micrographs for (a) as-deposited and (b) annealed at 500 °C for 3 h TiO<sub>2</sub> films obtained at the shown deposition temperature,  $T_s$ .

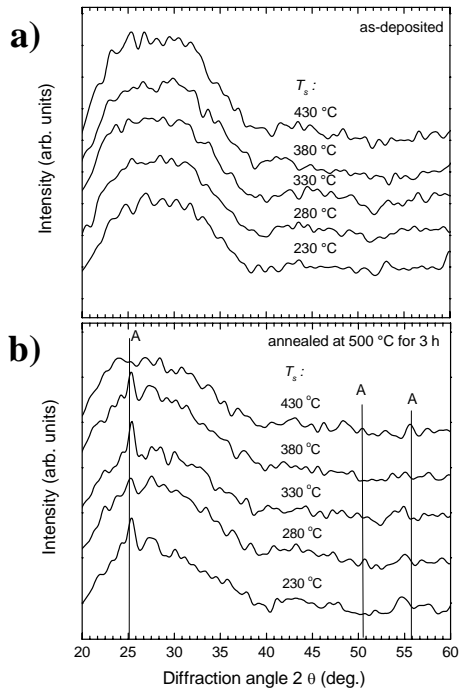


**Figure 4.** XDR patterns for (a) as-deposited and (b) annealed at 500 °C for 3 h TiO<sub>2</sub> films obtained the shown deposition temperature,  $T_s$ . The letter A denote the anatase phase peaks.

### 3.2 Optical Characterization

The optical transparency of the titanium dioxide thin films (Fig. 6) change depending the deposition temperature  $T_s$ , film thickness and structural configuration. In order to characterize the optical transparency we have used the luminous transmittance,  $T_{lum}$ , which is the ratio of the luminous flux transmitted by the film to the incident luminous flux, taking into account the spectral luminous efficiency of the eye in daylight [36]:

$$T_{lum} = \frac{\int T(\lambda) \Gamma_e(\lambda) d(\lambda)}{\int \Gamma_e(\lambda) d(\lambda)} \quad (2)$$

Here,  $T(\lambda)$  is the optical transmittance and  $\Gamma_e$  is a weighting function for the response of the human eye. Fig. 6 displays  $T_{lum}$  of as-deposited and annealed TiO<sub>2</sub> films as a function of substrate temperature,  $T_s$ . The maximum  $T_{lum}$  for as deposited is at  $T_s = 350$  °C, whereas the annealed films shows a maximum  $T_{lum}$  at  $T_s = 380$  °C.

The transparency of the as-deposited films (figure 6) increases with the deposition temperature. Transparent films were obtained at 330 and 380 °C, whereas highly diffuse films were obtained at 230, 280 and 430 °C. The films with high diffusivities in air is attributed to the light scattering due to roughness of the films; an alternative explanation could be the phase changes near to 400 °C in the substrate temperature [33] during the annealing process [34]. For both as-deposited and annealed samples, the transparency behaviors are in agreement with the results obtained in the roughness analysis (Fig. 2).

### 3.3 Photocatalytic characterization

The relative concentration,  $C/C_0$ , of methylene-blue in water as a function of the irradiation time for as-deposited and annealed TiO<sub>2</sub> films are shown in Fig. 7. The initial methylene-blue concentration in aqueous solution,  $C_0$ , was 20 ppm. The as-deposited film prepared at 280 °C has the best degradation efficiency, 25 %, (Fig. 7a). The films annealed at 500 °C for 3 h show less variation respect to the as-deposited films in the photocatalytic activity, the annealed films obtained at higher  $T_s$  than 280 °C improved their photo catalytic efficiency respect to that of the as-deposited films (Fig. 7b). Therefore for those films, the heat treatment improves the photocatalytic activity of the as-deposited TiO<sub>2</sub> which can be ascribed mainly due to the transformation of TiO<sub>2</sub> films to crystalline anatase phase [37]. Those films prepared at  $T_s=280$  °C and  $T_s=230$  °C presented a decrement of their photocatalytic activity, when they are heat treated which can be ascribed to a reduction of the active surface area as a consequence of the coalescence of the particles, promoted by the annealing. On the other hand, the cracks formed (see figure 3b) can be poisoned due to its high chemisorptions level [33], which decreases the photocatalytic activity because either the other reactant molecule cannot react with the MB or the MB molecules or the by products of the reaction are immobilized inside the porous [38].



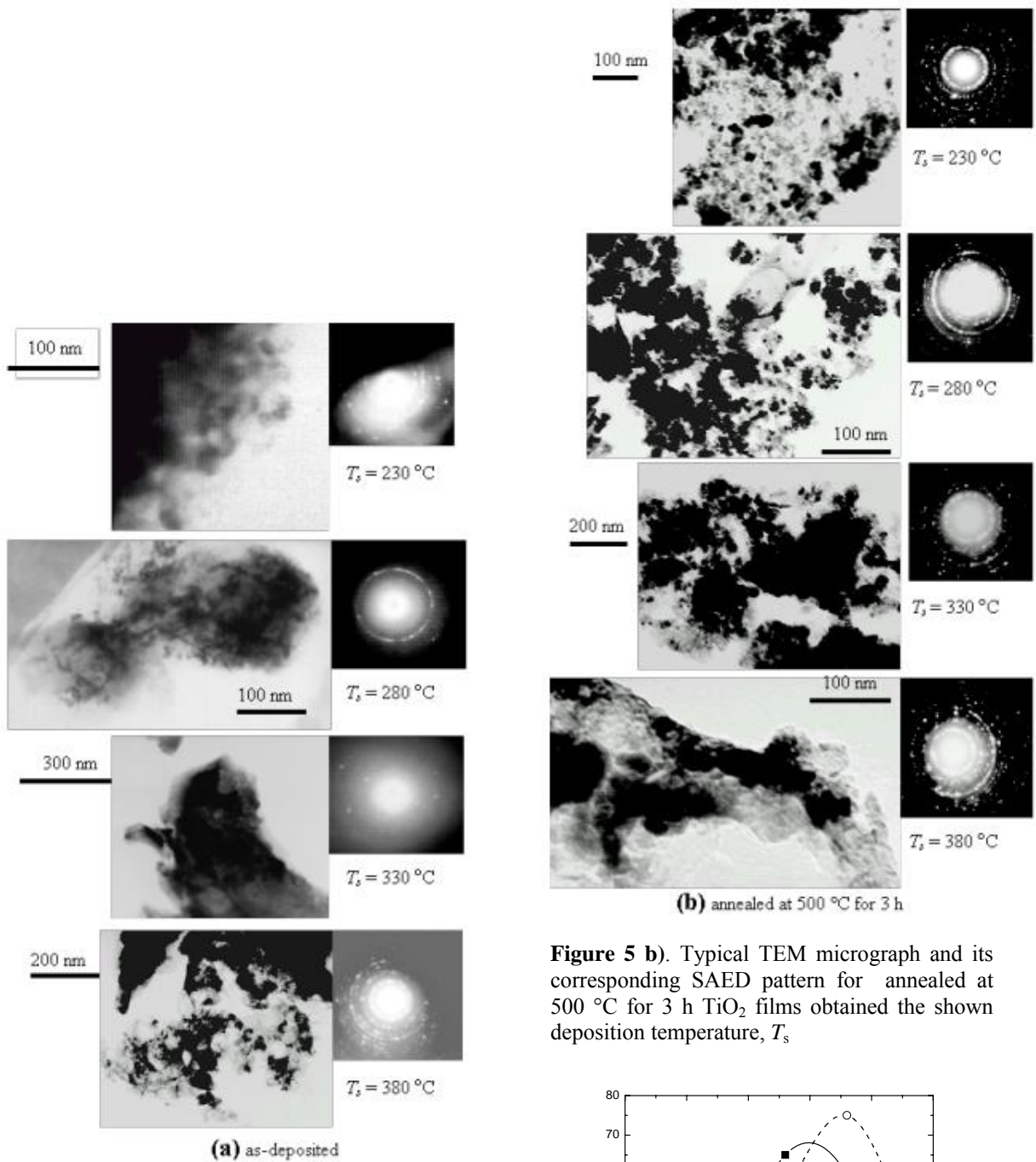


**Figure 5 a).** Typical TEM micrograph and its corresponding SAED pattern for (a) as-deposited TiO<sub>2</sub> thin films obtained the shown deposition temperature,  $T_s$

**Figure 5 b).** Typical TEM micrograph and its corresponding SAED pattern for annealed at  $500$  °C for 3 h TiO<sub>2</sub> films obtained the shown deposition temperature,  $T_s$

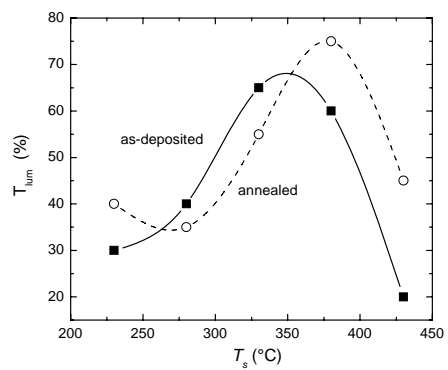


**Figure 6.** Luminous transmittance  $T_{lum}$  for as-deposited (■) and annealed at  $500$  °C for 3 h (○) TiO<sub>2</sub> deposited at different substrate temperatures. Symbols denote data and the curves were drawn for convenience.

**Table 1.** Pseudo-first order rate constants ( $k$ ) and pseudo-first order rate constant ( $k_s$ ) per unit of surface area obtained from the least square fitting of the semi-logarithmic plots of concentration ratio ( $C_0/C$ ) as a function of irradiation time.

Substrate temp. ( $^{\circ}\text{C}$ )	As-deposited Samples		Annealed Samples	
	$k$ ( $\text{h}^{-1}$ )	$k_s$ ( $\text{h}^{-1}\text{m}^{-2}$ )	$k$ ( $\text{h}^{-1}$ )	$k_s$ ( $\text{h}^{-1}\text{m}^{-2}$ )
230	0.025	62.50	0.017	42.50
280	0.046	115.00	0.037	92.00
330	0.013	32.50	0.023	57.50
380	0.007	17.50	0.023	57.50
430	0.007	17.50	0.023	57.50

The rate constant  $k$  and  $k_s$  of photocatalytic decomposition reaction obtained from the linear relationship of logarithms of relative concentration of MB with the irradiation time are listed in Table 1. It can be seen that the  $k_s$  value for as-deposited  $\text{TiO}_2$  film obtained with  $T_s=280\text{ }^{\circ}\text{C}$  ( $115.00\text{ h}^{-1}\text{m}^{-2}$ ) is the highest.

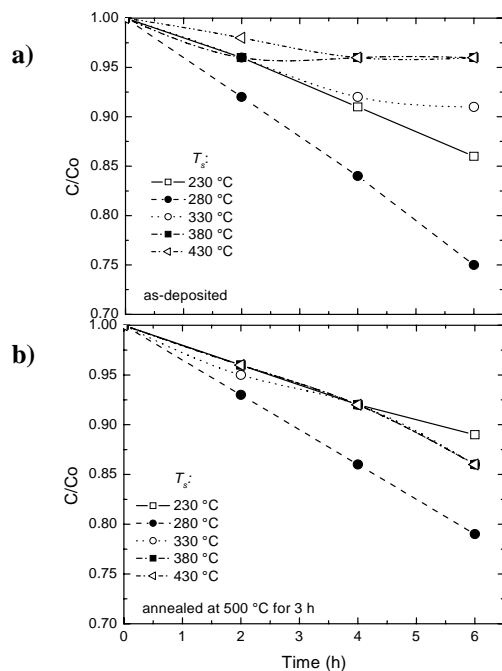


**Figure 7.** Relative concentration,  $C_0/C$ , as a function of irradiation time for (a) as-deposited and (b) annealed at  $500\text{ }^{\circ}\text{C}$  for 3 h  $\text{TiO}_2$  films.  $C_0$  is the initial concentration of methylene-blue of 20 ppm.

The annealing process increases the rate constant  $k_s$  for  $\text{TiO}_2$  films obtained with  $T_s$  higher than  $280\text{ }^{\circ}\text{C}$ . After annealing  $k_s$  increases 1.76 and 3.38 times for  $\text{TiO}_2$  films obtained with  $T_s = 330\text{ }^{\circ}\text{C}$ , and  $T_s = 380\text{ }^{\circ}\text{C}$  -  $430\text{ }^{\circ}\text{C}$ , respectively. However, it should be

pointed out that evaluation of rate constant can serve as guidance for the different systems (geometric configuration, illumination intensity, contaminant concentration, catalyst quantity, films thickness, etc.).

#### 4. Conclusions

The feasibility of depositing transparent nanocrystalline structure of the  $\text{TiO}_2/\text{glass}$  thin films has been successfully prepared by pulsed spray pyrolysis technique from a peroxo-titanium complex dissolved in ethanol. This method is simple, quick, safe, cost-effective and reproducible. The as-deposited samples did not show any XRD diffraction peaks; and crystallizes to anatase phase after annealing at  $500\text{ }^{\circ}\text{C}$  for 3 h. The SAED patterns from the as-deposited samples shows the presence of a few segregates of brookite phase with an average grain size  $\sim 7.5\text{ nm}$  and after the annealing process at  $500\text{ }^{\circ}\text{C}$  for 3 h the structure becomes to a polycrystalline anatase phase with an average grain size of  $\sim 10\text{ nm}$ .

Photocatalytic activity of the nanostructured- $\text{TiO}_2$  obtained by spray depends on morphology characteristics of the films. We found that  $\text{TiO}_2$  film obtained at  $280\text{ }^{\circ}\text{C}$  has the optimal photo catalytic processes for degrading methylene-blue in water. The low deposition temperature ( $280\text{ }^{\circ}\text{C}$ ) gives the possibility to use flexible polymer as substrates. These results support the viability of the SP technique and may expand to decomposition of other pollutants in water and also in gaseous state, though still experimental examinations are desired. The as-deposited  $\text{TiO}_2$  thin films prepared at  $280\text{ }^{\circ}\text{C}$  could be use in a cost-efficient solar water treatment process.

#### 5. Acknowledgments

The authors are grateful to J. Cañetas, J. G. Morales, C. Magaña, M. Aguilar, Dr. J. M. Hernandez and Dr. H. Murrieta from IFUNAM, Dr. A. Ortiz from IIM, to CONACYT and DGAPA-UNAM from Mexico, for the support in the projects 34821-E and IN109500 respectively. One of us (A. L.) wants to thank to Dr. W. Estrada, J. Rodriguez and J. Solis for fruitful discussion.

## 6. References

1. A. Fujishima, K. Hashimoto, and T. Watanabe, *TiO<sub>2</sub> Photocatalysis Fundamentals and Applications*. (BKC Inc., Japan, 1999).
2. T. Kodas and M. J. Hampden-Smith. *Aerosol Processing of Materials*. (Wiley-VCH, U.S.A., 1999).
3. D. Dvoranová, V. Brezová, M. Mazúr, and M. A. Malati, *Appl. Catal. B* 37 (2002) 91.
4. W. H. Leng, Z. Zhang, and J. Q. Zhang, *J. Mol. Catal. A* 2006 (2003) 239.
5. M. Gomez, J. Rodriguez, S. Tingry, A. Hagfeldt, S. E. Lindquist, and C. G. Grandvist, *Sol. Energy Mater. Sol. Cells* 59 (1999) 277.
6. M. Kitao, Y. Oshima, and K. Urabe, *Jpn. J. Appl. Phys.* 36 (1997) 4423.
7. D. Bhattacharyya, N. K. Sahoo, S. Thakur, and N. C. Das, *Thin Solid Films* 360 (2000) 96.
8. M. Miki-Yoshida, V. Collins-Martínez, P. Amézaga-Madrid, and A. Aguilar-Elguézabal, *Thin Solid Films* 419 (2002) 60.
9. A. B. R. Mayer; W. Grebner, and R. Wannemacher, *J. Phys. Chem. B*, 104 (2000) 72.
10. H. Tamai, T. Ikeya, F. Nishiyama, H. Yasuda, K. Tida, and S. Nojima, *J. Mater. Sci.* 25 (2000) 4945.
11. T. Torimoto, Y. Okawa, N. Takeda, and H. Yoneyama, *J. of Photobiology A: Chem.* 103 (1997) 153-157.
12. A. Mills, N. Elliott, I. P. Parkin, S. A. O'Neill, and R. J. Clark. *Photochem. Photobiol. A* 151 (2002) 171.
13. C. Li, G. Yang, and Z. Wang, *Mater. Lett.* 57 (2003) 2130.
14. M. Hirasawa, T. Seto, T. Orii, N. Aya, and H. Shimura *Appl. Phys. Sci.* 197-198 (2002) 661.
15. C. Legrand-Buscema, C. Malibert, and S. Bach, *Thin Solid Films* 418 (2002) 79.
16. H. Lin, H. Kozuka, and T. Yoko, *Thin Solid Films* 315 (1998) 111.
17. M.C. Barnes, A.R. Gerson, S. Kumar, and N.-M. Hwang, *Thin Solid Films* 446 (2004) 29.
18. P. Zeman and S. Takabayashi, *Surf. Coat. Technol.* 153 (2002) 93.
19. L. Sirghi, T. Aoki, and Y. Hatanaka, *Thin Solid Films* 422 (2002) 55.
20. S. H. Oh, D. J. Kim, S. H. Hahn, and E. J. Kim, *Mater. Lett.* 57 (2003) 4151.
21. H. Shin, R. J. Collins, M. R. De Guire, A. H. Heuer, and C. N. Sukemik, *J. Mater. Res.* 10 (1995) 692.
22. D. Mergel, D. Buschendorf, S. Eggert, R. Grammes, and B. Samset, *Thin Solid Films* 371 (2000) 218.
23. J. M. Nedelj Kovic, Z. V. Saponjic, Z. Rakocevic, V. Jocanovic, and D. P. Uskokovic, *Nanostructured Mater.* 9 (1997) 125.
24. P.P. Ahonem, E. I. Kaupinen, J. C. Joubert, J. L. Deschanvres, and G. Van Tenedlo, *J. Mater. Res.*, 14 (1999) 3938.
25. G. L. Messing, S. Zhang and G. V. Jayanthi, *J. Am. Ceram. Soc.* 76 (1993) 2707.
26. J. Lee, H. Cho, and S. Park. *Ceramic Powder Sci. IV* (1992) 39.
27. M. O. Abou-Helal, and W. T. Seeber *Appl. Surf. Sci.* 195 (2002) 53.
28. F. Di Muzio, M. Masi, and S. Carrà. *Mater. Chem. Phys.* 66 (2000) 286.
29. C. Natarajan, N. Fukunaga, and G. Nogami, *Thin Solid Films* 322 (1998) 6.
30. A. I. Martinez, D. Acosta, *Thin Solid Films*, to be published.
31. M. Toyoda, Y. Nanbu, Y. Nakasawa, M. Hirano, M. Inagaki, *App. Catálisis B: Environmental* 49 (2004) 277.
32. L. Castañeda, J.C. Alonzo, A. Ortiz, E. Andrade, J. M. Saniger, J. G. Bañuelos, *Mat. Chem. And Physics* 77 (2002) 938.
33. M. Blesa (Ed.), *Monografía: Eliminación de contaminantes por fotocátalisis heterogénea*, Red Temática CYTED, Argentina 2001.
34. A. Conde-Gallardo, M. Guerrero, N. Castillo, A. B. Soto, R. Frago, J. G. Cabañas-Moreno *Thin Solid Films* 473 (2005) 68-72.
35. Relva C. Buchanam and Taeun Park *Materials Crystal Chemistry* Marcel Dekker Inc. USA 1997
36. M. Gómez, J. Lu, J. L. Solis, E. Olsson, A. Hagfeldt, and C. G. Granqvist. *J. Phys. Chem. B*, 104 (2000) 8712.
37. J. Yu, X. Zhao, and Q. Zhao, *Mater. Chem. Phys.* 69 (2001) 25
38. P. W. Atkins, *Physical Chemistry*, Oxford University Press, Oxford, UK 1995.